

REGULAR PAPERS

Synthesis and investigation of anchoring unit effect in blue-colored isoindigo-based D–A– π –A organic dyes for dye-sensitized solar cells

To cite this article: Chang Hee Son *et al* 2018 *Jpn. J. Appl. Phys.* **57** 122302

View the [article online](#) for updates and enhancements.



Synthesis and investigation of anchoring unit effect in blue-colored isoindigo-based D–A– π –A organic dyes for dye-sensitized solar cells

Chang Hee Son^{1†}, Suresh Thogiti^{1†}, Ramesh Kumar Chitumalla², Ganesh Koyyada^{1*}, Rajesh Cheruku¹, Joonkyung Jang², Jae Hak Jung^{1*}, and Jae Hong Kim^{1*}

¹Department of Chemical Engineering, Yeungnam University, Gyeongsan, Gyeongbuk 712-749, Republic of Korea

²Department of Nanoenergy Engineering, Pusan National University, Busan 609-735, Republic of Korea

*E-mail: ganeshkoyyada@ynu.ac.kr; jhjung@ynu.ac.kr; jaehkim@yumail.ac.kr

[†]These authors contributed equally to this work.

Received August 30, 2018; accepted October 3, 2018; published online November 16, 2018

Isoindigo-based blue colored organic dyes (IND-B, IND-T, and IND-I) with different electron acceptors such as 2-cyanoacetic acid/carboxylated 1,3-indandione bridged through benzene or thiophene π -spacers were synthesized and applied in dye-sensitized solar cells (DSSCs). The photoelectrochemical performances and charge transport properties revealed that the device fabricated with IND-B sensitizer showed the highest power conversion efficiency of 3.37% among the three dyes. The diminished performance of IND-T and IND-I is partially attributed to the relatively lower lying LUMO level. The designated charge transport of the synthesized dyes secured from electrochemical impedance spectroscopy (EIS) analysis were found to be in accordance with experimentally attained photovoltaic parameters. © 2018 The Japan Society of Applied Physics

1. Introduction

Dye-sensitized solar cells (DSSCs) have attracted considerable interest in both academic and industrial communities since the innovative work by Graetzel group in 1991, owing to their low cost and ease fabrication.¹ Narrow band gap dye chromophores are found to be a promising strategy for advancement of high-performance DSSCs due to their wide-band spectral response.^{2,3} In this respect, organic dye chromophores are predicted to be ideal alternatives due to their easy tuning of the energy band gap and the high light harvesting ability as compared to traditional metal (Ru)-based complexes.^{4–7} Isoindigo is a structural isomer of the well-known pigment indigo, and is often found as an intermediate in drug development.⁸ Due to the electron-deficient properties and planar π -conjugation, isoindigo units were successfully combined with electron-rich donor units to build low band-gap polymer semiconductors used in bulk heterojunction organic solar cells.⁹ In the past few years, the photovoltaic performance of isoindigo-based DSSCs has been recorded and the best power conversion efficiency (PCE) of 7.55% has been attained.^{10–15} Recently, Li et al. tested that a bis[4-(*tert*-butyl)phenyl]amine donor, directly connected to an electron-deficient isoindigo group, is more favorable for electron communication in D– π –A frame as compared to the triphenylamine unit.

Nowadays, a D–A– π –A structure for metal-free organic dyes was described and attained growing attention with an electron pulling chromophore introduced into the common D– π –A configuration by incorporating the subordinate acceptor. This acts as an electron trap to separate charge and promote electron transfer to the final acceptor, the sensitizer displays broad responsive spectra.^{15–18} On the other hand, there are few reports on the effect of different electron acceptor/anchoring on the D–A– π –A organic molecular structure. In these organic dyes, cyanoacetic acid is commonly introduced into D–A– π –A configuration as an anchoring group.

Recently, D– π –A configuration containing a carboxylated 1,3-indandione anchoring unit, DN475, has been communicated to perform PCE of 5.76% on a plastic substrate.¹⁹ This

unit was first introduced by Shoji et al. in 2012 as one of anchoring unit with greater electron withdrawing ability to study the photovoltaic performance in DSSCs.²⁰ Matsui et al. utilized this carboxylated 1,3-indandione anchoring unit and one of the dyes attained a notable efficiency of 6.11%.²¹ Herein, for DSSC applications, we synthesize novel blue colored isoindigo-based D–A– π –A dyes for which the charge chromophoric system consists bis[4-(*tert*-butyl)phenyl]amine as the common donor with two different anchoring units. Benzene and thiophene conjugate groups are introduced between the donor–acceptor and acceptor units as the π -spacers to extend the π -conjugation, which is expected to further increase the light harvesting ability. Figure 1 displays the corresponding dye structures.

2. Experimental methods

2.1 Instruments and measurements

All ¹H NMR spectra were recorded on a Varian Mercury NMR 300 MHz spectrometer using CDCl₃ and DMSO-d₆, which were both purchased from Alfa Aesar. The chemical shifts were referenced to TMS. The absorption spectra were recorded on an Agilent 8453 UV–vis spectrophotometer. The redox properties of three dyes were examined by using cyclic voltammetry (CV; BAS Epsilon). The electrolyte solution used was 0.10 M tetrabutylammonium hexafluorophosphate (TBABF₆) in freshly dried dichloromethane. The Ag/AgCl and Pt wire (0.5 mm in diameter) electrodes were used as reference and counter electrodes, respectively. The scan rate was 30 mV/s. The electrochemical impedance spectroscopy (EIS) was performed using an electronic-chemical analyzer (Iviumstat Tec.). The photovoltaic current–voltage (*I*–*V*) characteristics of the prepared DSSCs were measured under 1 sunlight intensity (100 mW cm^{–2}, AM1.5), which was verified with an AIST-calibrated Si-solar cell (Peccell Technologies PEC-L11). The incident monochromatic photon-to-current efficiencies (IPCEs) were plotted as a function of the light wavelength using an IPCE measurement instrument (Peccell Technologies PEC-S20).

2.2 Synthesis of sensitizers

All commercially available starting materials and solvents were purchased from Aldrich, Alfa, TCI, and ACROS and

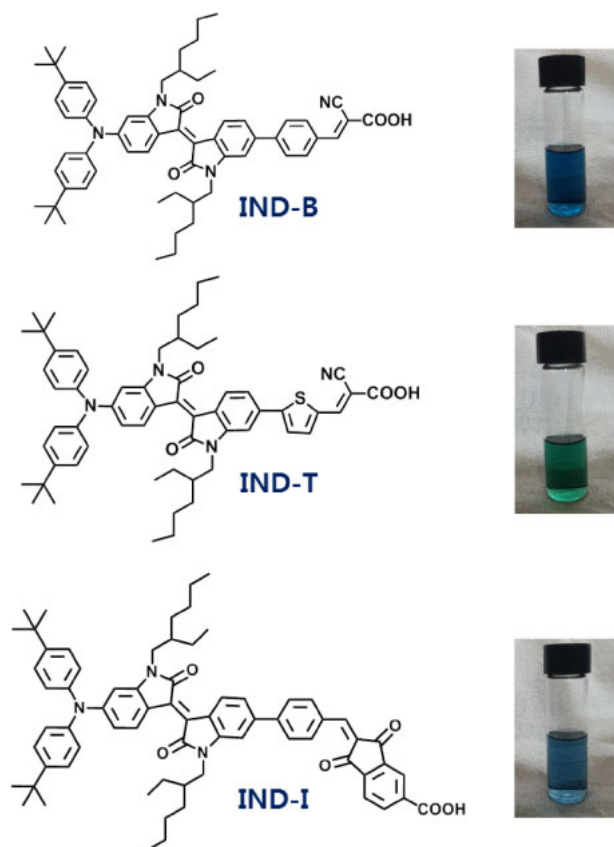


Fig. 1. (Color online) Molecular structure of synthesized dye-sensitizers IND-B, IND-T, and IND-I.

used as received. The synthetic procedures were performed according to the literature method.¹⁰ The synthesis of two new organic sensitizers was carried out according to Fig. 2 (procedures documented in the online supplementary data at <http://stacks.iop.org/JJAP/57/122302/mmedia>).

2.3 Computational details

All the reported density functional theory (DFT) calculations were performed with Gaussian 09 quantum chemical program.²² The structures were constructed and the output files were visualized and analyzed using GaussView software.²³ We optimized the ground state geometries of the three dyes by employing a hybrid B3LYP^{24,25} functional in combination with 6-31G(d) basis set. Vibrational frequency analysis was carried out to confirm the real minima on the potential energy surface. The minima were confirmed with no imaginary frequencies. The optimized geometries of the dyes were used to simulate their UV–visible absorption spectra. The optical spectra were simulated by employing time-dependent (DFT) TDDFT formalism. The experimental solvent conditions were mimicked by using polarizable continuum model to define dichloromethane solvent. The TDDFT simulations were performed at PBE0/6-31G(d) level of theory.²⁶

3. Results and discussion

Figure 3(a) shows the optical absorption spectra of the dye molecules measured in dichloromethane solutions and Table I lists the data. As shown in Fig. 3(a), IND-B showed an absorption maximum at 610 nm. Compared to the λ_{\max} of IND-B, the absorption pattern of IND-T was red-shifted by

25 nm, with λ_{\max} at 635 nm because of the replacement of benzene spacer with heteroaromatic thiophene spacer. IND-I including carboxylated 1,3-indandione as an acceptor showed a red-shift in their absorption spectrum compared to the 2-cyanoacetic acid-based dyes IND-B and IND-T. This red shift can be attributed to the extension of the π -conjugation and stronger electron pulling ability of carboxylated 1,3-indandione. The blue shift of the absorption spectra of the dyes on semiconductor TiO₂ [Fig. 3(b)] was ascribed to deprotonation of the H-type aggregation/carboxylic acid. From Fig. 3(a), E_{0-0} values of 1.69, 1.63, and 1.56 eV were calculated for IND-B, IND-T, and IND-I, respectively.

The CVs of dyes were obtained in a 0.1 M *n*-Bu₄NPF₆ in dichloromethane solution. The data were used to calculate the energy of the highest occupied molecular orbital (HOMO) and the lowest unoccupied molecular orbital (LUMO) to investigate the regeneration of the dyes from the redox electrolyte and charge transfer from the excited dye-sensitizer to the conduction band of the TiO₂, respectively. Herein, the onset oxidation potentials of oxidation peak of CV traces were used to compute the HOMO level using the following formula:

$$\text{HOMO} = -[E_{\text{onset}}^{\text{oxd}} - 4.7 \text{ eV}], \quad (1)$$

where $E_{\text{onset}}^{\text{oxd}}$ stands for the onset oxidation potential. The optical bandgap E_{0-0} values are obtained from the onset absorption spectra [Fig. 3(a)]. The E_{0-0} and HOMO values were used to calculate their LUMO energy levels; the values in volts (V) against NHE were converted into electron volts (eV) according to the following formula:

$$\text{LUMO} = [\text{HOMO} - E_{0-0}] \text{ eV}. \quad (2)$$

It is well known that the action of effective electron injection and dye regeneration is extremely depends on the position of LUMO and HOMO energy levels with respect to the conduction band of TiO₂ and redox potential of electrolyte.^{27,28} The HOMO, LUMO, and E_{0-0} values are listed in Table I. The HOMO levels of the IND-B, IND-T, and IND-I dyes were noticed to be -5.71 , -5.73 , and -5.70 eV, respectively; these values are more positive than that of the I⁻/I₃⁻ redox electrolyte (-5.2 eV).²⁹ This suggests that the oxidized dye can be regenerated via electron donation from the I⁻ ions in the iodine-based redox electrolyte. The LUMO values (Table I) of IND-B, IND-T, and IND-I were calculated to be -4.02 , -4.10 , and -4.14 eV, respectively.

The electron-pulling units have a considerable effect on the reduction potentials of the dyes and the stronger electron-pulling capability corresponds to a less negative reduction potential or lower lying LUMO energy. When the dye's LUMO is situated near the energy level of the conduction band edge of TiO₂ semiconductor, charge injection from the excited state of the dye into the conduction band of TiO₂ is thermodynamically less feasible. In this case, charge transfer from the excited dye to the semiconductor conduction band (-4.2 eV)²⁹ becomes energetically less favored in a situation that would result in strong recombination. The energy level diagrams pertaining to the optical and cyclic voltammetry studies are represented in Fig. 4. Surprisingly, IND-T and IND-I, which had better absorption spectral properties than IND-B dye, exhibits lowered LUMO level. Particularly, LUMO level of IND-I was almost identical with the con-

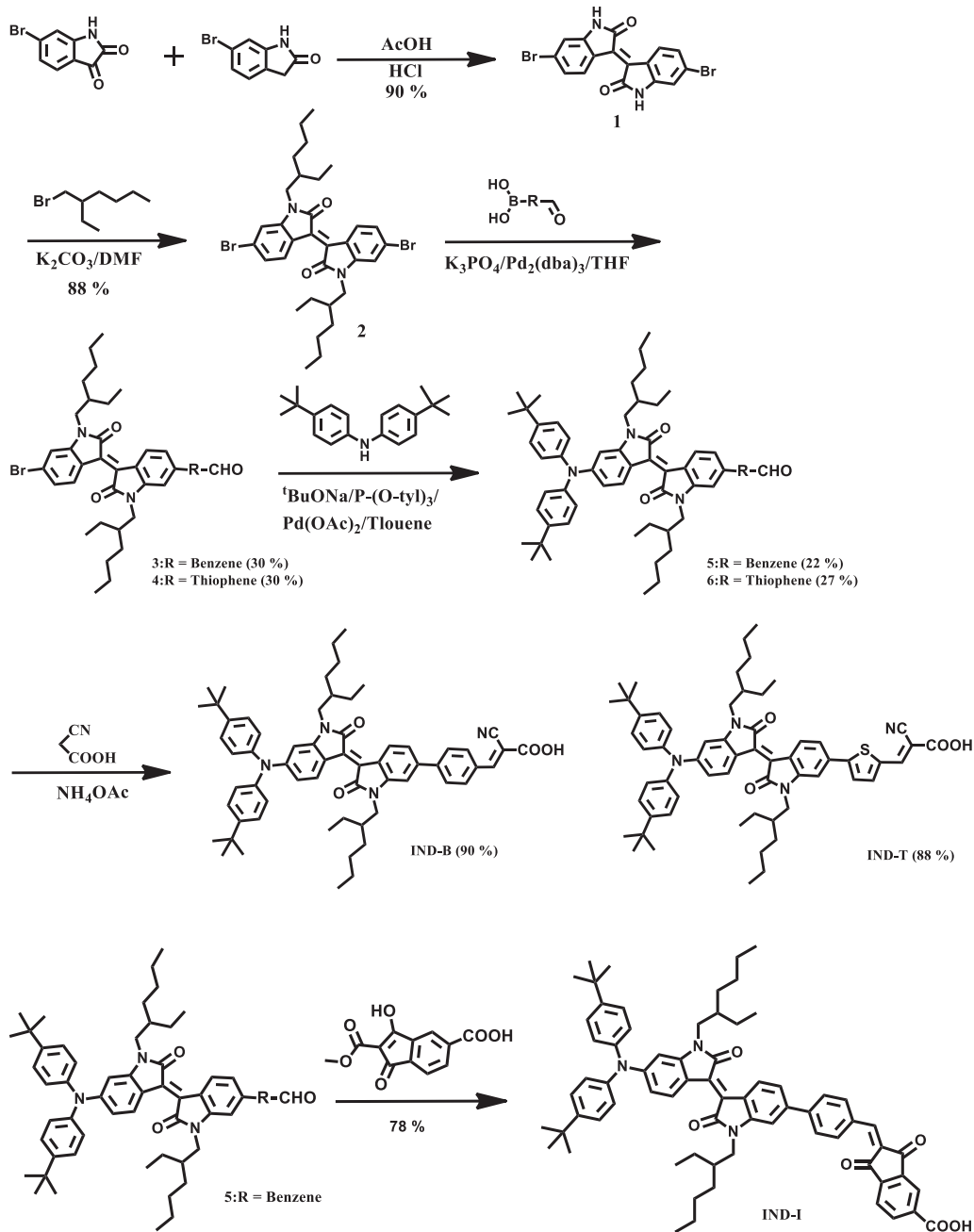


Fig. 2. Synthesis of IND-B, IND-T, and IND-I dyes.

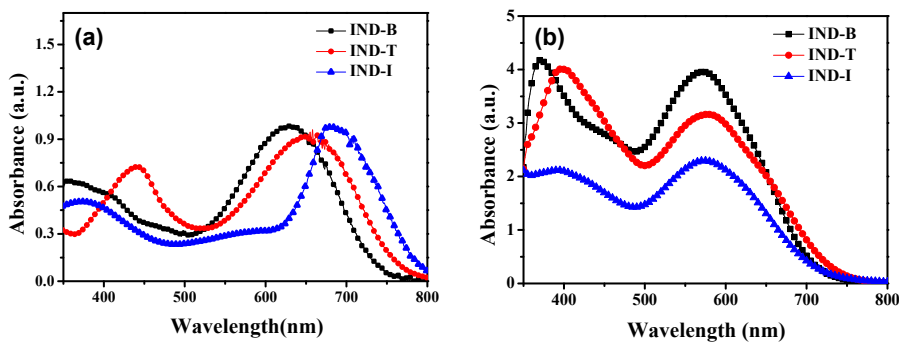


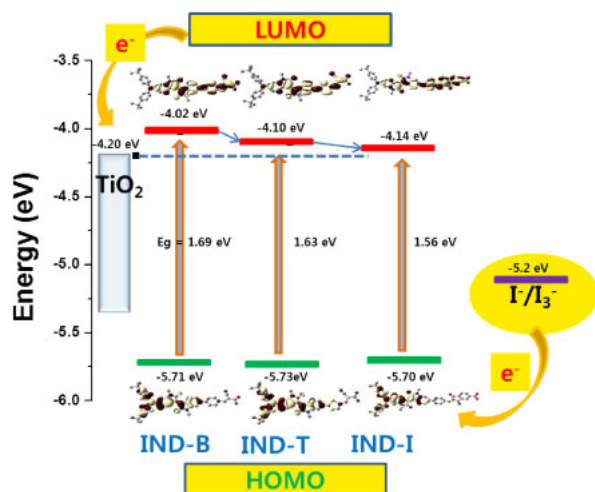
Fig. 3. (Color online) Absorption spectra of the dyes in (a) dichloromethane solution, (b) on TiO₂ films.

duction band of TiO₂. On the other hand, the negative free energies for electron injection were obtained from the difference between the LUMO level of dyes and the conduction

band edge of TiO₂. Their negative free energy values were shown to be in the order: IND-B (0.18 eV) > IND-T (0.1 eV) > IND-I (0.06 eV). From the results, it is clear that the

Table I. Photophysical and electrochemical data for IND dye sensitizers.

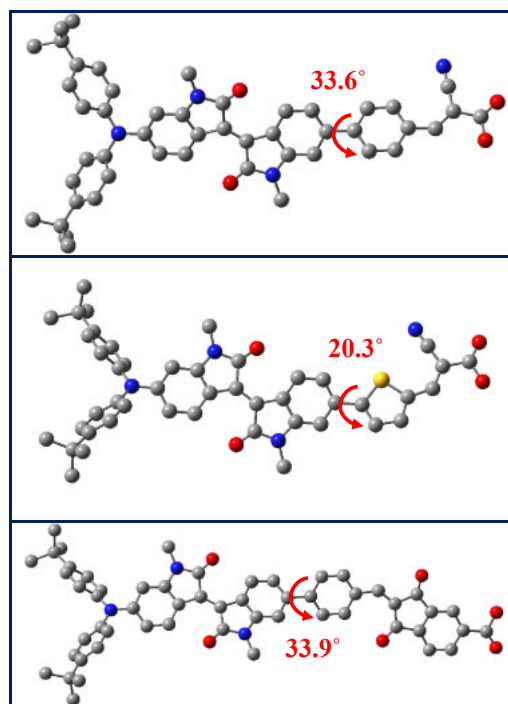
Dye	λ_{\max} (nm)		E_{ox} (V)	E_{0-0} (eV)	E_{ox}^* (V)	HOMO (eV)	LUMO (eV)
	Solution	TiO ₂					
IND-B	610	572	1.01	1.69	-0.68	-5.71	-4.02
IND-T	635	578	1.03	1.63	-0.60	-5.73	-4.10
IND-I	710	573	1.00	1.56	-0.56	-5.70	-4.14

**Fig. 4.** (Color online) Energy level diagram of IND-B, IND-T, and IND-I dyes.

dyes IND-T and IND-I would be less efficient for electron injection into the conduction band of TiO₂ than the IND-B. Consequently, this phenomenon could result in strong recombination currents, degrading the photovoltaic performance of IND-T and IND-I compared to the dye IND-B. Previously, density functional theory calculations showed that isoindigo-based dyes with strong electron acceptor near the anchoring unit could decrease the LUMO level of the dyes, which could lead to the less thermodynamic driving force for electron injection into the TiO₂.¹⁴ For comparison, optical and electrochemical data of structurally similar dye ICD-3 were shown in Table I.¹⁰ In a study of the energy bandgap of TiO₂, the LUMO level of TiO₂ could be decreased by doping metal atom into TiO₂, so we could consider it to solve the low LUMO level of the dyes.³⁰

We have performed the computational investigation to theoretically characterize the novel blue colored three organic dyes. As the alkyl group on nitrogen have very marginal effects on optical and electrochemical behavior, we have modeled the dyes IND-B, IND-T, and IND-I by replacing the lengthy alkyl chain on nitrogen with a simple methyl group to save the computational time. The substituted two indolin moieties are in planar and the attached π -spacers (phenyl/thiophene) are deviating slightly from the planarity. The dihedral angles of the π -spacers with Indolin are calculated to be 33.6, 20.3, and 33.9° for IND-B, IND-T, and IND-I, respectively. The optimized ground state geometries of the dyes and the calculated dihedral angles are shown in Fig. 5.

The population analysis of the dyes revealed the electron density distribution in the frontier molecular orbitals of the dyes. In HOMO, the electron density is predominantly localized over triphenylamine and indolin moieties. Whereas, in the LUMOs, the electron density has been shifted towards

**Fig. 5.** (Color online) Optimized ground state molecular geometries of the dyes IND-B (top), IND-T (middle), and IND-I (bottom) obtained at B3LYP/6-31G(d) level of the theory.

spacer and anchoring groups. The shifting of electron density from the donor (triphenylamine) to anchoring groups through the spacers facilitates the electron injection. Figure 6 depicts the calculated electron density distribution pattern in the HOMO and LUMO. The HOMO values of all the three dyes have been found to be similar around -5.33 eV and the LUMO values are -3.40, -3.49, and -3.42 eV for IND-B, IND-T, and IND-I, respectively. The theoretical electrochemical data are in good agreement with those obtained from the experimental CV. The simulated absorption spectra of the dyes in dichloromethane solvent have been depicted in Fig. 7 and the optical data have been summarized in Table II. The calculated excitation energies of the dyes IND-B, IND-T, and IND-I are 1.93, 1.84, and 1.89 eV and the corresponding absorption wavelengths are 642, 672, and 656 nm, respectively. The lowered LUMO of the IND-T is responsible for its redshifted absorption in the UV-visible spectra compared to that of IND-B. The simulated absorption maxima of IND-B and IND-T are slightly overestimated and IND-I is slightly underestimated when compared with those of experiment. The deviation in calculated optical properties of the dyes with those of experiment is attributed to the modifications made in the modeling of the dyes and also to the inherent limitations in the TDDFT methodology.³¹

Table III presents the device performance data under AM 1.5 illuminations. Figures 8(a) and 8(b) show the incident photon-to-current conversion efficiencies (IPCE) and the photocurrent-voltage (J - V) curves of the devices, respectively. The PCEs of the DSSC devices fabricated and measured under similar conditions ranged from 0.4 to 3.37%. For comparison, the photovoltaic performance of the structurally similar dye ICD-3 included in Table II.¹⁰ The large difference in the overall PCE comes mainly from the difference in the current densities between them. The device with IND-B

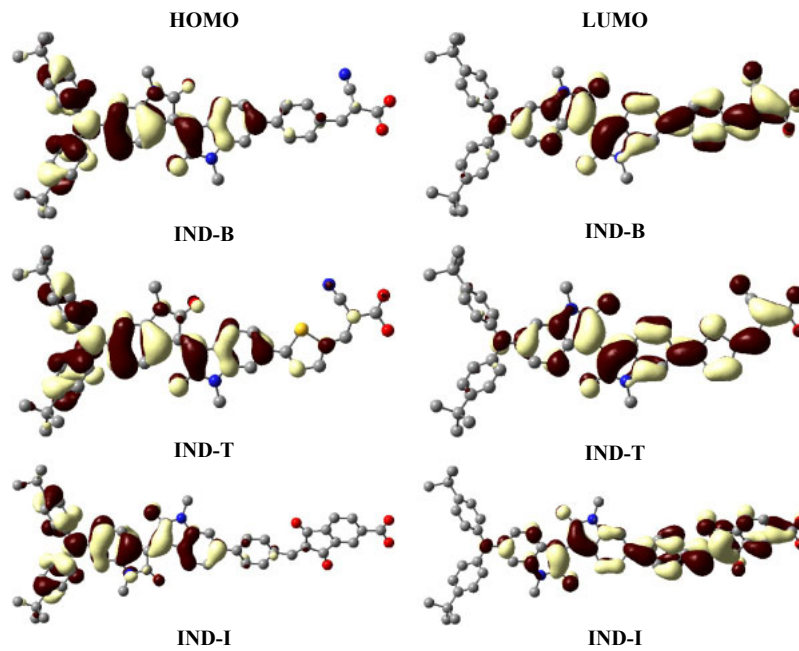


Fig. 6. (Color online) Calculated electron density distribution in frontier molecular orbitals of the dyes IND-B, IND-T, and IND-I.

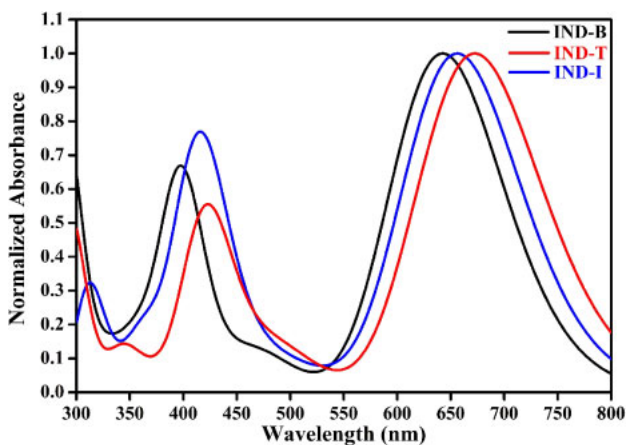


Fig. 7. (Color online) Simulated absorption spectra of the dyes IND-B, IND-T, and IND-I in dichloromethane at B3LYP/6-31G(d) level of the theory.

Table II. Calculated optical and electrochemical data of the dyes IND-B, IND-I, and IND-T.

Dye	HOMO (eV)	LUMO (eV)	Excitation energy (eV)	Oscillator strength f	Major transition (%)
IND-B	-5.33	-3.40	1.93	1.1624	HOMO \rightarrow LUMO (95)
IND-T	-5.33	-3.49	1.84	1.8441	HOMO \rightarrow LUMO (96)
IND-I	-5.31	-3.42	1.89	1.2594	HOMO \rightarrow LUMO (90)

Table III. Photovoltaic data for the DSSCs based on IND dye sensitizers and reference N719.

Dye	J_{sc} (mA cm ⁻²)	V_{oc} (V)	FF (%)	η (%)
N719	14.62	0.65	67.59	6.42
IND-B	8.78	0.66	57.91	3.37
IND-T	5.34	0.58	65.56	2.05
IND-I	1.26	0.50	68.84	0.4

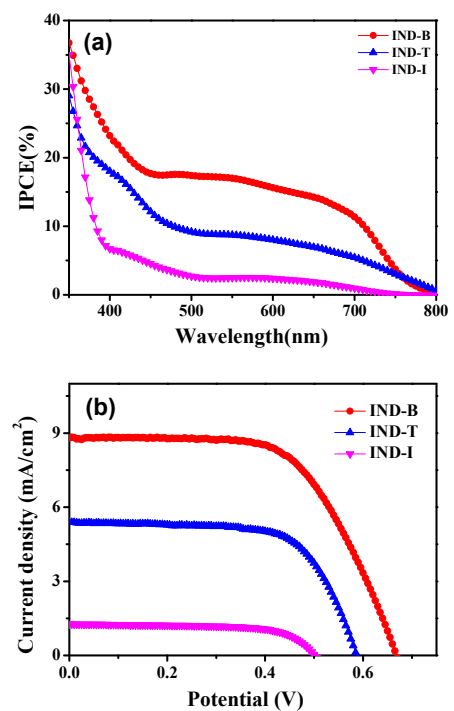


Fig. 8. (Color online) (a) Spectra of IPCE and (b) J - V characteristics of the different IND dyes.

having benzene as π -spacer showed higher V_{oc} than device with thiophene π -spacer in IND-T. Although better electron accepting unit render IND-I with better light harvesting properties than IND-B and IND-T, IND-I still showed the lowest PCE among all the devices due to decreased IPCE and V_{oc} values. The highest cell efficiency of IND-B was attributed to absorption and the IPCE of IND-B was intense both in the solution and on the TiO₂ film and has the highest J_{sc} and V_{oc} values. Dyes IND-B and IND-T with cyanoacetic acid as acceptor exhibited a stronger solar cell response [Fig. 8(a)] in the 400–800 nm spectral regions compared to

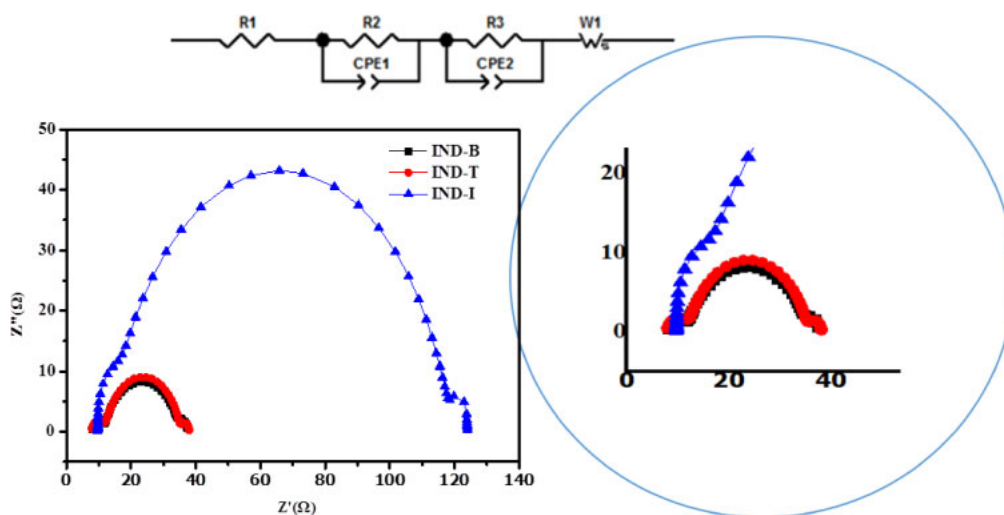


Fig. 9. (Color online) Nyquist plots and equivalent circuits (top) for DSSCs based on IND dyes measured under illumination conditions.

Table IV. Electrochemical impedance parameters (in Ω) of DSSCs based on dye sensitizers IND-B, IND-T, and IND-I.

Dye	R_1	R_2	R_3	W_s
IND-B	7.99	3.58	23.72	2.3
IND-T	7.66	4.46	25.28	2.6
IND-I	9.62	4.33	104.8	5.4

that of IND-I. Under the same conditions, the N719-based DSSC gave a J_{SC} of 14.62 mA cm^{-2} , a V_{OC} of 0.65 V , a FF of 67.59% , and a PCE of 6.42% .

EIS of the DSSCs based on different dyes was performed to shed further light on the difference in the photovoltaic performance between the dye sensitized solar cells. As shown in Fig. 9, two semicircles were observed in the Nyquist plots. The smaller and larger semicircles in the Nyquist plots were assigned to charge transfer at the counter electrode/electrolyte interface and the TiO_2 /dye/electrolyte interface, respectively. The W_s at lower frequency indicates diffusion of the redox shuttle through the electrolyte. R_1 is the series resistance, R_2 is the resistance of electron transport in the counter electrode, and R_3 is the charge transfer resistance between the TiO_2 film and the electrolyte.^{32,33} Table IV summarizes the fitting results. The values of R_3 of these dyes were in the order of $\text{IND-I} > \text{IND-T} > \text{IND-B}$. Clearly, a lower R_3 value was obtained for the dye containing cyanoacetic acid as the anchoring group. The introduction of carboxylated indandione as anchoring group largely increases the electron transfer resistance. For IND-B and IND-T, the values of R_3 were 23.72 and 25.28Ω , respectively whereas the R_3 value of IND-I was 104.8Ω . An increase in the R_3 value would result in a diminished performance, i.e., photo-regeneration is more ineffective. The fitting data of EIS agreed well with the cell efficiency shown in Fig. 8 and Table III.

4. Conclusions

For application in dye-sensitized solar cells, we have synthesized novel blue colored organic dyes; each contains a bis[4-(*tert*-butyl)phenyl]amine as common electron donor and cyanoacetic acid or carboxylated 1,3-indandione electron acceptor linked by benzene or thiophene groups serving as

π -conjugated bridges. To increase the power conversion efficiency, our target here is to extend the absorption region to longer wavelengths. The overall PCE of the device based on IND-B with cyanoacetic acid anchoring unit (3.37%) was higher than that of other dyes. Despite extended absorption region to longer wavelength, the device with IND-T and IND-I showed decreased IPCE values, possibly due to the lower lying LUMO level and/or charge entrapment around the strong electron withdrawing group. Electrochemical impedance analysis revealed that the device with IND-I showed increased charge transfer resistance, rendering a decrease in overall efficiency.

Acknowledgment

This work was supported by the 2015 Yeungnam University Research Grant.

- 1) B. O'Regan and M. Grätzel, *Nature* **353**, 737 (1991).
- 2) J. H. Yum, E. Baranoff, S. Wenger, M. K. Nazeeruddin, and M. Graetzel, *Energy Environ. Sci.* **4**, 842 (2011).
- 3) S. K. Balasingam, M. Lee, M. G. Kang, and Y. Jun, *Chem. Commun.* **49**, 1471 (2013).
- 4) M. K. Nazeeruddin, F. De Angelis, S. Fantacci, A. Selloni, G. Viscardi, P. Liska, S. Ito, B. Takeru, and M. Graetzel, *J. Am. Chem. Soc.* **127**, 16835 (2005).
- 5) T. H. Nguyen, T. Suresh, and J. H. Kim, *Org. Electron.* **30**, 40 (2016).
- 6) F. Gao, Y. Wang, D. Shi, J. Zhang, M. Wang, X. Jing, P. Humphry-Baker, S. Wang, M. Zakeeruddin, and M. Gratzel, *J. Am. Chem. Soc.* **130**, 10720 (2008).
- 7) K.-J. Jiang, N. Masaki, J. Xia, S. Noda, and S. Yanagida, *Chem. Commun.*, 2460 (2006).
- 8) M. Sassatelli, F. Bouchikhi, B. Aboab, F. Anizon, D. Fabbro, M. Prudhomme, and P. Moreau, *Anticancer Drugs* **18**, 1069 (2007).
- 9) L. Fang, Y. Zhou, Y. X. Yao, Y. Diao, W. Y. Lee, A. L. Appleton, R. Allen, J. Reinspach, S. C. B. Mannsfeld, and Z. N. Bao, *Chem. Mater.* **25**, 4874 (2013).
- 10) S.-G. Li, K.-J. Jiang, J.-H. Huang, L.-M. Yang, and Y.-L. Song, *Chem. Commun.* **50**, 4309 (2014).
- 11) W. Gang, T. Haijun, Z. Yiping, W. Yingying, H. Zhubin, Y. Guipeng, and C. Pan, *Synth. Met.* **187**, 17 (2014).
- 12) R. Stalder, D. Xie, A. Islam, L. Han, J. R. Reynolds, and K. S. Schanze, *ACS Appl. Mater. Interfaces* **6**, 8715 (2014).
- 13) D. Wang, W. Ying, X. Zhang, Y. Hu, W. Wu, and J. Hua, *Dyes Pigm.* **112**, 327 (2015).
- 14) D. Y. Kwon, D. M. Chang, and Y. S. Kim, *Mater. Res. Bull.* **58**, 93 (2014).
- 15) W. Ying, F. Guo, J. Li, Q. Zhang, W. Wu, H. Tian, and J. Hua, *ACS Appl.*

- [Mater. Interfaces](#) **4**, 4215 (2012).
- 16) J. Mao, J. Y. Guo, F. L. Ying, W. J. Wu, W. J. Li, and J. Hua, [Chem.—Asian J.](#) **7**, 982 (2012).
- 17) W. Q. Li, Y. Z. Wu, Q. Zhang, H. Tian, and W. H. Zhu, [ACS Appl. Mater. Interfaces](#) **4**, 1822 (2012).
- 18) K. Pei, Y. Wu, W. Wu, Q. Zhang, B. Chen, H. Tian, and W. H. Zhu, [Chem.—Eur. J.](#) **18**, 8190 (2012).
- 19) N. Shibayama, Y. Inoue, M. Abe, S. Kajiyama, H. Ozawa, H. Miura, and H. Arakawa, [Chem. Commun.](#) **51**, 12795 (2015).
- 20) S. Matsumoto, T. Aoki, T. Suzuki, M. Akazome, A. Betto, and Y. Suda, [Bull. Chem. Soc. Jpn.](#) **85**, 1329 (2012).
- 21) M. Matsui, R. Kimura, Y. Kubota, K. Funabiki, K. Manseki, J. Jin, A. Hansuebsai, Y. Inoue, and S. Higashijima, [Dyes Pigm.](#) **147**, 50 (2017).
- 22) M. J. Frisch, G. W. Trucks, H. B. Schlegel, G. E. Scuseria, M. A. Robb, J. R. Cheeseman, G. Scalmani, V. Barone, B. Mennucci, G. A. Petersson, H. Nakatsuji, M. Caricato, X. Li, H. P. Hratchian, A. F. Izmaylov, J. Bloino, G. Zheng, J. L. Sonnenberg, M. Hada, M. Ehara, K. Toyota, R. Fukuda, J. Hasegawa, M. Ishida, T. Nakajima, Y. Honda, O. Kitao, H. Nakai, T. Vreven, J. A. Montgomery, J. E. Peralta, F. Ogliaro, M. Bearpark, J. J. Heyd, E. Brothers, K. N. Kudin, V. N. Staroverov, R. Kobayashi, J. Normand, K. Raghavachari, A. Rendell, J. C. Burant, S. S. Iyengar, J. Tomasi, M. Cossi, N. Rega, J. M. Millam, M. Klene, J. E. Knox, J. B. Cross, V. Bakken, C. Adamo, J. Jaramillo, R. Gomperts, R. E. Stratmann, O. Yazyev, A. J. Austin, R. Cammi, C. Pomelli, J. W. Ochterski, R. L. Martin, K. Morokuma, V. G. Zakrzewski, G. A. Voth, P. Salvador, J. J. Dannenberg, S. Dapprich, A. D. Daniels, O. Farkas, J. B. Foresman, J. V. Ortiz, J. Cioslowski, and D. J. Fox, Gaussian 09 (Wallingford, CT, 2009).
- 23) R. Dennington, T. Keith, J. Millam, K. Eppinnett, W. L. Hovell, and R. Gilliland, GaussView, Version 4.1 (Semichem, Inc., Shawnee Mission, KS, 2003).
- 24) A. D. Becke, [J. Chem. Phys.](#) **98**, 5648 (1993).
- 25) A. D. Becke, [J. Chem. Phys.](#) **104**, 1040 (1996).
- 26) J. P. Perdew, K. Burke, and M. Ernzerhof, [Phys. Rev. Lett.](#) **77**, 3865 (1996).
- 27) T. Suresh, G. Rajkumar, S. P. Singh, P. Y. Reddy, A. Islam, L. Han, and M. Chandrasekharam, [Org. Electron.](#) **14**, 2243 (2013).
- 28) T. Suresh, K. Ganesh, S. P. Singh, A. Islam, L. Han, and M. Chandrasekharam, [Dyes Pigm.](#) **99**, 850 (2013).
- 29) T. Suresh, R. K. Chitumalla, N. T. Hai, J. Jang, T. J. Lee, and J. H. Kim, [RSC Adv.](#) **6**, 26559 (2016).
- 30) W. Wang, H. Zhang, L. Wu, J. Li, Y. Qian, and Y. Li, [J. Alloys Compd.](#) **657**, 53 (2016).
- 31) S. Grimme and M. Parac, [ChemPhysChem](#) **4**, 292 (2003).
- 32) H. J. Ahn, S. Thogiti, J. M. Cho, B. Y. Jang, and J. H. Kim, [Electron. Mater. Lett.](#) **11**, 822 (2015).
- 33) C. T. T. Thuy, J. H. Jung, S. Thogiti, W.-S. Jung, K.-S. Ahn, and J. H. Kim, [Electrochim. Acta](#) **205**, 170 (2016).